

Sequence-to-Label Script Identification for Multilingual OCR

Yasuhisa Fujii*, Karel Driesen*, Jonathan Baccash, Ash Hurst, Ashok C. Popat
 Google Research, Mountain View, CA 94043, USA
 {yasuhisaf,karel,jbaccash,phurst,popat}@google.com

Abstract—We describe a novel line-level script identification method. Previous work repurposed an OCR model generating per-character script codes, counted to obtain line-level script identification. This has two shortcomings. First, as a *sequence-to-sequence* model it is more complex than necessary for the *sequence-to-label* problem of line script identification. This makes it harder to train and inefficient to run. Second, the counting heuristic may be suboptimal compared to a learned model. Therefore we reframe line script identification as a *sequence-to-label* problem and solve it using two components, trained *end-to-end*: *Encoder* and *Summarizer*. The encoder converts a line image into a feature sequence. The summarizer aggregates the sequence to classify the line. We test various summarizers with identical inception-style convolutional networks as encoders. Experiments on scanned books and photos containing 232 languages in 30 scripts show 16% reduction of script identification error rate compared to the baseline. This improved script identification reduces the character error rate attributable to script misidentification by 33%.

I. INTRODUCTION

Multilingual optical character recognition (OCR), where the scripts and languages of input images are unknown, is a challenging problem in OCR. This holds in particular for multi-script images. Most existing systems assume scripts to be known in advance and do not handle mixed or misspecified scripts gracefully. Ideally, OCR should work fast and accurately with or without script specification.

A straightforward approach to handle arbitrary scripts and languages is to cover all of them by one model. The resulting mammoth system recognizes text in a broad range of scripts, but this universality can cost accuracy and speed. Alternatively, we can model each individual script or language and use model selection as a first stage. Genzel et al. presented a multilingual OCR system based on line-level script identification where each script and language has its own OCR model [1]. We adopt a similar approach. However, we use a coarser, script-based model taxonomy where a model recognizes any language in a given script. Section II describes our multilingual OCR system. Note that selection is done at the text-line level, i.e. each line is assumed to be in a single script. Section VI discusses this choice. We use script identification for OCR model selection. Therefore, it is a crucial component of the system.

Script identification as a *pixels-to-label* problem is a well-studied topic. Early efforts focused on scanned documents with white background and excellent resolution [2]. Recent efforts deal with messier video and still camera images [3], [4].

*: These authors contributed equally.

We perform script identification on an entire text line. At the line level we can exploit the sequential nature of written text, similar to speech recognition. [1], [5] use sequence models for line-level script identification by framing the problem as a *sequence-to-sequence* problem. In contrast, we frame the problem as a conceptually simpler *sequence-to-label* problem. We propose to model it with two components trained *end-to-end*. The first component is an *Encoder* to convert a line image to a sequence of features. The second component is a *Summarizer* to take the feature sequence and produce a single classification. Similar formulations appear in [4] for script identification of scene texts and in [6], [7] for speaker identification and verification in speech processing. We design and evaluate various summarizers with an inception-style [8] convolutional network-based encoder in Section III.

II. MULTILINGUAL OCR

A. Overview

Fig. 1 shows our multilingual OCR system. The first step extracts text lines from the image. This step may provide structural layout information on paragraphs or sections. It can also provide stylistic information such as bold or italic style, as described in [9]. Next, script identification selects a script-specific OCR model among 30 scripts. See Table II. The script-specific OCR model then produces a unicode transcription of the line image. Finally, the recognition results further enhance layout analysis (Post-recognition Layout Analysis). For example, mistakes in the initial layout are corrected post OCR by using a low recognition confidence as a signal that an initial text box was not actually text.

We focus on script identification and text line recognition, treating text line detection as given. Section III describes the details of script identification methods.

B. Text Line Recognition with Script Identification

Text line recognition takes a text line image as input and produces a sequence of Unicode code points, for example represented as UTF-8 strings. Let x be an input line image and y be a sequence of code points. We employ a probabilistic approach to model the relationship and consider the conditional probability $P(y|x)$. Let $s \in S$ be a script. The

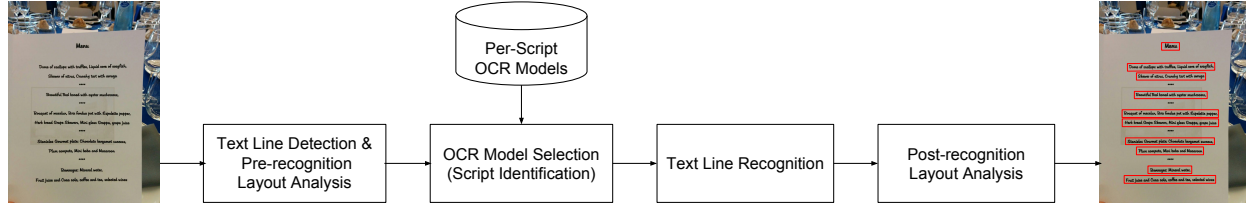


Fig. 1. Multilingual OCR system with line-level script identification.

script information is incorporated into $P(\mathbf{y}|\mathbf{x})$ by considering s as a hidden variable. We compute $P(\mathbf{y}|\mathbf{x})$ as follows:

$$\begin{aligned} P(\mathbf{y}|\mathbf{x}) &= \sum_s P(\mathbf{y}, s|\mathbf{x}) \\ &= \sum_s P(\mathbf{y}|s, \mathbf{x})P(s|\mathbf{x}) \\ &\approx P(\mathbf{y}|\arg\max_s P(s|\mathbf{x}), \mathbf{x}). \end{aligned} \quad (1)$$

$P(\mathbf{y}|s, \mathbf{x})$ represents an OCR model of a script s . $P(s|\mathbf{x})$ represents a script identifier, which is described in Section III. Note that the formulation employs hard classification and only considers the script which maximizes $P(s|\mathbf{x})$ in text recognition. The limitation of this approach is discussed in Section VI.

We use the following approximation to compute $P(\mathbf{y}|s, \mathbf{x})$:

$$\begin{aligned} P(\mathbf{y}|s, \mathbf{x}) &= \frac{P(\mathbf{y}|s, \mathbf{x})}{P(\mathbf{y}|s)} P(\mathbf{y}|s) \\ &\approx \prod_{i=1}^{|C(\mathbf{y})|} \frac{P(c_i|s, \mathbf{x})}{P(c_i|s)} P(\mathbf{y}|s) \end{aligned} \quad (2)$$

where $C(\mathbf{y})$ is a function to convert \mathbf{y} to a corresponding sequence of grapheme clusters $(c_1, c_2, \dots, c_{|C(\mathbf{y})|})$, and where c_i is the i -th grapheme cluster of \mathbf{y} . $P(c_i|s, \mathbf{x})$, $P(c_i|s)$ and $P(\mathbf{y}|s)$ are an optical model, a prior probability of a grapheme cluster c , and a language model, respectively, for a script s . In practice, we combine these probabilities by taking the logarithms and using the values as the scores in a log-linear model. We use a log-linear model framework as in [10].

We model $P(c_i|s, \mathbf{x})$ with a neural network. We assume that \mathbf{x} is a tensor representing an image of fixed-height and has shape (h, w, d) where h represents the fixed-height, w is the width and d is the number of channels of the image. We fix the height to 40 and collapse the color space down to luminance (grayscale). We use an inception-style convolutional neural network as in [8] to convert \mathbf{x} into a tensor representing a sequence of frames of shape (w', d') where w' is the length of the sequence and d' is the dimensionality of features, see Fig. 2. Fig. 3 shows the complete topology of our model. Connectionist temporal classification (CTC) [11] computes $\prod_i^{C(\mathbf{y})} P(c_i|s, \mathbf{x})$ from the output.

We use different models for horizontal and vertical texts of the same script. To deal with both directions uniformly we rotate vertical texts 90 degrees counterclockwise and make

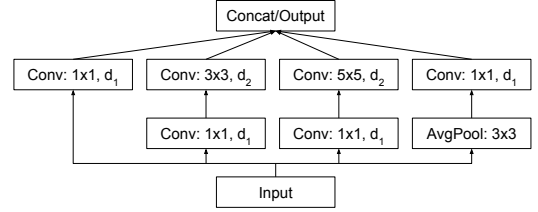


Fig. 2. Inception module used in the paper. “Conv: $h_f \times w_f, d$ ” represents a convolutional neural network layer where h_f , w_f , and d mean the height of filter, the width of filter and the number of filters, respectively. The activation function is $\text{relu6}(x) = \min(\max(0, x), 6)$. “AvgPool: $h_f \times w_f$ ” represents an average pooling layer. The stride of filters is always 1×1 for both layers. “Concat” concatenates all the inputs along the last dimension. The SAME padding is used for all operations.

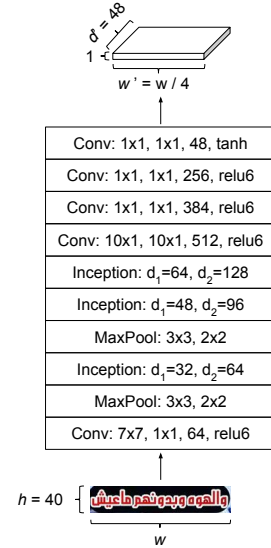


Fig. 3. Topology of the optical model. “Conv: $h_f \times w_f, h_s \times w_s, c, f$ ” represents a convolutional neural network layer where h_f , w_f , h_s , w_s , c and f mean the height of filter, the width of filter, the shift in the height dimension, the shift in the width dimension and the number of filters and the activation function, respectively. $\tanh(x) = (1 - \exp(-2x))/(1 + \exp(-2x))$. “Max-Pool: $h_f \times w_f, h_s \times w_s$ ” represents a max pooling layer. “Inception: d_1, d_2 ” represents an inception module that is defined in Fig. 2. The SAME padding is used for all operations.

them visually horizontal. See Fig. 7 for an example. Right-to-left languages (e.g. Hebrew, Arabic) do not need special handling since text line recognition deals with a line image as a whole. Frames are offered to the network in display order.

$P(c|s)$ is the unigram language model of grapheme clusters

and mathematically needed to use the optical model $P(c|s, \mathbf{x})$ with the language model $P(\mathbf{y}|s)$ [12]. We estimate the probability by computing the moving average of $P(c|s, \mathbf{x})$ during training.

$P(\mathbf{y}|s)$ is modeled as an N -gram language model defined over Unicode points. We use (with pruning) $N = 9$ for all scripts except Chinese, Japanese and Korean for which we use $N = 4$. Note that the script s may be used to represent multiple languages. Therefore “language model” in the foregoing should be understood in the functional sense of capturing the known prior statistical regularity of the strings to be recognized, rather than referring to a single actual language.

III. LINE-LEVEL SCRIPT IDENTIFICATION

Line-level script identification takes a line image as input and produces a script code. We model the relationship with a probability $P(s|\mathbf{x})$. Since \mathbf{x} is inherently a sequence, we solve the problem as a sequence-to-label problem with two components that are trained end-to-end: *Encoder* and *Summarizer*. Encoders are used to convert a line image into a sequence of features and summarizers are used to aggregate the sequence to perform the classification. Fig 4 visualizes the concept. An encoder $E(\mathbf{x})$ takes \mathbf{x} as input and outputs a sequence of features \mathbf{h} that is a tensor of shape (w', d') where w' is the length and d' is the dimensionality of the features. A summarizer $F(\mathbf{h}, s)$ transforms the feature sequence into a set of scalar values, one for each script s . These values are then transformed via *softmax* into the posterior distribution $P(s|\mathbf{x})$ with $E(\mathbf{x})$ and $F(\mathbf{h}, s)$:

$$P(s|\mathbf{x}) = \frac{\exp(F(E(\mathbf{x}), s))}{\sum_{s'} \exp(F(E(\mathbf{x}), s'))}. \quad (3)$$

We train all model variations using cross-entropy loss. The following sections describe the encoder and summarizers considered in this work.

A. Encoder

We use the inception-style convolutional neural network shown in Fig. 3 as the encoder for all summarizers. It is identical to the encoder layer of the OCR network described in Section II-B. This allows a fair comparison between all summarizer variants. Note that further optimization is possible: we can reduce the number of parameters (e.g. fewer channels in every convolutional layer) without hurting accuracy since classification to 30 scripts needs fewer parameters than accurate character recognition for a line of symbols.

B. Summarizer

1) *Max*: The Max summarizer produces a tensor of shape $(|S|)$ for each index of a sequence \mathbf{h} and takes the maximum per script over the sequence which has w' values for each script. We represent the function to compute the tensor of shape $(w', |S|)$ from \mathbf{h} as $L(\mathbf{h})$. We model $L(\mathbf{h})$ with a neural network and use the topology shown in Fig. 5a. Formally, we define the summarizer as follows:

$$F^{\max}(\mathbf{h}, s) \stackrel{\text{def}}{=} \max_i l_{i,s}, \quad (4)$$

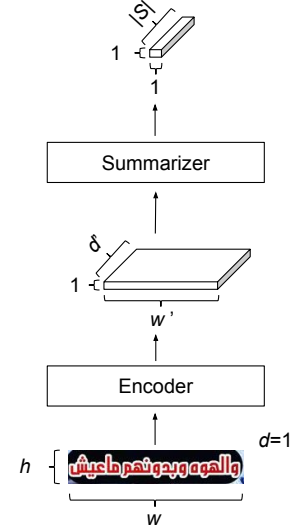


Fig. 4. The encoder-summarizer framework to solve script identification as a sequence-to-label problem. An encoder processes an input of shape (h, w, d) and produces an output of shape (w', d') . A summarizer produces an output of shape $(|S|)$. Encoders and summarizers are typically modeled by neural networks and are trained end-to-end.

where $\mathbf{l}_{*,s} = (l_{1,s}, l_{2,s}, \dots, l_{w',s}) = L(\mathbf{h})$.

2) *Mean*: The Mean summarizer computes the mean of $L(\mathbf{h})$ for each script as follows:

$$F^{\text{mean}}(\mathbf{h}, s) \stackrel{\text{def}}{=} \frac{1}{|\mathbf{l}_{*,s}|} \sum_i l_{i,s}. \quad (5)$$

Max and Mean summarizers correspond to the methods proposed in [4].

3) *Gate*: The Gate summarizer computes the mean of $L(\mathbf{h})$ for each script as the Mean summarizer does. However, it also utilizes an attention-like gating mechanism to select indices which should be considered in the final output. We denote a function as $G(\mathbf{h})$ to convert a tensor of shape (w', d') to a tensor of shape (w') . We model $G(\mathbf{h})$ with a neural network and use the topology shown in Fig. 5b. Formally, we define the summarizer as follows:

$$F^{\text{Gate}}(\mathbf{h}, s) \stackrel{\text{def}}{=} \frac{1}{\sum_i g_i} \sum_i g_i \cdot l_{i,s}, \quad (6)$$

where $\mathbf{g} = (g_1, g_2, \dots, g_{w'}) = G(\mathbf{h})$.

4) *LSTM*: In [13], long short-term memory (LSTM) [14] is used to encode a sequence of inputs to a single output. Similar techniques can be used to formulate a summarizer. The LSTM summarizer uses a forward LSTM followed by a backward LSTM to aggregate the sequence. Both forward and backward LSTMs consume a sequence and produce another sequence. We use the values at the first index of the output of the backward LSTM as the aggregated values. We further apply a sequence of fully-connected layers to obtain the final output of shape $(|S|)$. We represent these operations as $M(\mathbf{h})$.

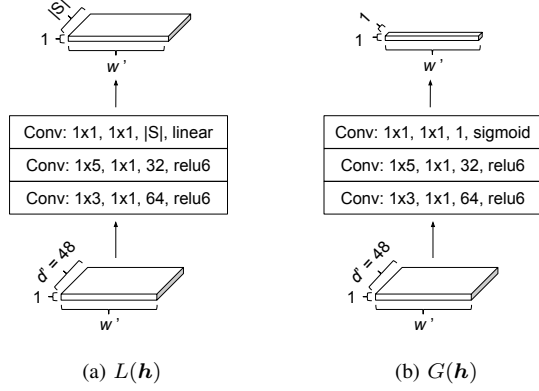


Fig. 5. Topology of $L(\mathbf{h})$ and $G(\mathbf{h})$. $\text{linear}(x) = x$. $\text{sigmoid}(x) = 1/(1 + \exp(-x))$. The SAME padding is used for all operations. See Fig. 3 for the other notations.

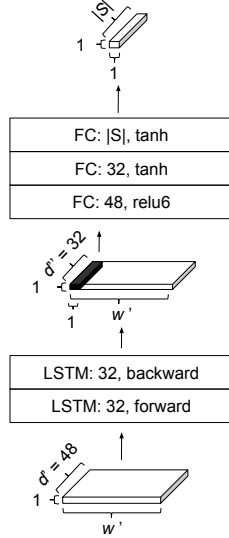


Fig. 6. Topology of $M(\mathbf{h})$. “LSTM: n, d ” represents an LSTM layer with n nodes in the direction d . “FC: n, f ” represents a fully-connected layer with n nodes and an activation function f . The values at the first index of the output of the backward LSTM are used as the aggregated values (depicted in black).

The topology of $M(\mathbf{h})$ is shown in Fig. 6. Formally, we define the summarizer as follows:

$$F^{\text{LSTM}}(\mathbf{h}, s) \stackrel{\text{def}}{=} l_s^{\text{LSTM}}, \quad (7)$$

where $l^{\text{LSTM}} = M(\mathbf{h})$.

C. Baseline

The OCR system described in Section II-B is repurposed for script identification as proposed in [1] by training it to output script codes instead of characters (1 per character). We implemented exactly the heuristic described in [1] to determine the *dominant script* of a line from the sequence of script codes. This heuristic gives each character a vote. Majority decides a unique script label per line. Some characters such as spaces and digits are ignored. Characters common in Japanese,

Encoder		Weights
Summarizers	Gate	39,968
	Lstm	23,103
	Sum	20,479
	Max	20,479

TABLE I
MODEL SIZES



Fig. 7. Examples of text line images from different domains.

Chinese Simplified and Chinese Traditional count towards all 3 scripts. Full details can be found in [1]. We refer to this baseline method as *Base* in the following sections.

D. Model Sizes

Table I shows model sizes. All models have close to 3 million weights. Most are used by the convolutional layers in the Encoder. The same Encoder is used between all end-to-end models. It is identical to feature-producing network (prior to CTC) in the repurposed OCR model that provides per-character script codes in the Baseline system. Summarizers are small compared to overall model size. They account for around 1% of total parameter size.

IV. EVALUATION DATA AND METHOD

Fig. 7 shows examples of text line images from 3 domains. Books-horizontal contains dense, book-like lines from 30 scripts. Books-vertical has book-like vertical lines in Korean, Japanese, and Chinese Traditional. While other languages also have vertical text, those characters are usually oriented perpendicular to the line. The line becomes horizontal after 90 degree rotation. Hence we only need separate script models

domain	scripts	langs	number of lines	
			eval	train
photos	Latin	1	9,235	192,383
	Cyrillic	1	3,981	0
	Japanese	1	2,863	0
	Arabic	1	2,442	0
	Devanagari	1	2,166	0
Sum	5	5	20,687	192,383
books vertical	Chinese Trad.	1	1,790	39,779
	Japanese	1	1,767	51,164
	Korean	1	921	37,644
Sum	3	3	4,478	128,587
books horizontal	Latin	163	61,883	62,649
	Cyrillic	28	24,088	92,530
	Devanagari	4	11,649	40,411
	Arabic	6	10,900	40,337
	Tibetan	2	8,860	15,125
	Syriac	1	3,370	14,893
	Hebrew	2	3,184	15,107
	Ethiopian	2	3,122	14,737
	Georgian	1	3,002	14,917
	Cherokee	1	2,935	14,610
	Bengali	2	2,809	14,819
	Myanmar	1	2,781	14,890
	Sinhala	1	2,493	15,005
	Oriya	1	1,626	15,226
	Thaana	1	1,363	14,526
	Lao	1	1,251	15,409
	Gujarati	1	1,184	14,807
	Gurmukhi	1	1,166	14,516
	Telugu	1	1,152	15,064
	Kannada	1	1,150	14,826
	Khmer	1	1,133	14,926
	Malayalam	1	1,124	14,795
	Thai	1	1,062	14,976
	Armenian	1	1,048	15,029
	Tamil	1	989	15,510
	Greek	2	932	15,016
	Korean	1	898	56,973
	Chinese Simpl.	1	834	63,474
	Japanese	1	802	62,134
	Chinese Trad.	1	796	57,429
Sum	30	232	159,586	804,666
Overall Sum	30	232	183,388	1,125,636

TABLE II
DATA DESCRIPTION

for truly vertical script with characters oriented along the line. The photos domain has text lines from photo-like images (e.g., born-digital, natural-scene). It is typically more challenging than book-like images.

Table II breaks down evaluation and training data. Non Latin scripts have fully synthetic training data. We digitally render text from Wikipedia and other web sources with added noise and distortion. For example, see the Zulu line in Fig. 7. Latin has in addition real, photo-like data from advertisements, for about 75% of total training data. Evaluation data is mostly non-synthetic. Model definition and training use TensorFlow [15].

Evaluation data has labeled real text line images from 232 languages in 30 scripts. Images come from web pages, smartphone photos, and book scans. Each labeled line image has transcribed text and bcp47 language code, which determines script label. 82K out of 183K lines in the horizontal books test set are synthetic. The other 101K are images of books or photos labeled by human raters. The 20K photo-like lines

	Confusions over 1%	
	Base	Gate
Latin	-	-
Cyrillic	Latin:4.2%	Latin:1.8%
Devanagari	-	-
Arabic	-	-
Tibetan	Latin:1.3%	-
Japanese	Chinese-Sim:1.9% Chinese-Tr:2.6%	Chinese-Tr:3.9%
Syriac	Latin:2.9% Arabic:1.2%	Latin:1.2% NonText:1.1%
Ethiopian	-	-
Hebrew	-	-
Georgian	-	-
Cherokee	Latin:5.2%	Latin:2.6%
Myanmar	-	-
Bengali	Latin:2.8%	Latin:1.6%
Chinese-Tr	Chinese-Sim:7.3%	-
Sinhala	-	-
Korean	Chinese-Tr:1.3%	Chinese-Tr:1.2%
Oriya	Latin:4.4%	Latin:2.2%
Thaana	-	-
Lao	Latin:3.5%	Latin:1.6% Telugu:1.4%
Gujarati	-	-
Gurmukhi	Arabic:2.4% Latin:1.8%	Arabic:2.5% Latin:1.1%
Telugu	-	-
Kannada	-	-
Khmer	Latin:15.7% Thai:2.6%	Latin:5.5% Lao:1.7%
Malayalam	Latin:1.2%	-
Greek	Latin:12.3%	Latin:1.4%
Thai	-	-
Armenian	Latin:21.1%	Latin:2.3%
Tamil	Latin:3.4%	-
Chinese-Sim	Chinese-Tr:1.7%	Chinese-Tr:3.7%

TABLE III
SCRIPT CONFUSIONS OVER 1% ON BOOKS DATA

in 5 languages/scripts are all human rated. 70% of supported languages use Latin script, but only 39% of evaluation text lines are Latin. Some scripts require more data, e.g. vertical Japanese or Arabic.

On script labels for multi-script lines: we first obtained a nominal language label by collecting test data in *a priori known* language corpuses. We then send text lines to language-capable human raters for verification of the language and script label. The raters also perform transcription of the text line. In some cases a line that is identified and confirmed to be in a particular language may contain a long phrase from a different script. To mitigate this issue we apply a filtering step in preparing our evaluation data. For example, we drop a line in the Japanese script eval set with less than 50% Japanese symbols (e.g. too much Latin text).

V. RESULTS

Table IV shows results for the 5 Script identification summarization techniques described in section III-B. We give the script identification error rate per domain. This is defined as number of lines in which script identification disagrees with the script label, divided by total number of lines. We also show OCR error rate due to script identification. This is end-to-end character error rate for the script identification technique

followed by our best per-script OCR model, subtracted by “Oracle-script” OCR error rate. This subtraction isolates OCR errors from script misidentification errors. The Oracle-script system simulates “perfect” script identification by using the script label. We show results for the photo domain, vertical book-like data for Korean/Japanese/Chinese Traditional, and horizontal book-like data.

Overall, the Gate system is the clear winner. Compared to Base it reduces script identification error rate by 16% relative (from 3.7% to 3.1%). The impact on end-to-end character recognition error from script misidentification goes down 33%, from 2.1% to 1.4%.

On subdomains, Gate beats other summarization methods with one exception. Max is slightly better on books-vertical, in particular on Korean. However, this does not result in significant character error rate reduction (0.1% on books-vertical). Overall, Max does not perform well. It is even slightly worse than Base on overall script identification error rate.

No technique beats all others on every script. Every technique achieves lowest script identification error on at least one script. Base wins on Latin, LSTM on Bengali, Mean on Cherokee, Max on Korean, and Gate on Khmer, among others. In aggregate all non-Base techniques excluding Max beat Base. Gate is the best among them.

Table III has the top script confusions¹ in books data per script for Base and Gate. We list all scripts accounting for more than 1% errors in any script. Mostly these are unsurprising. For instance Cyrillic has many characters that look like similar Latin characters. Japanese as well as Chinese Simplified retain the use of certain Chinese Traditional characters. Therefore these misidentifications are expected. Similarly, many non-Latin texts use Latin characters for names instead of transliterating. This explains Latin confusion. Gate gets rid of confusion or greatly diminishes it for all scripts except Chinese Simplified. The confusion with Chinese Traditional increases, congruent with the increased script identification error rate in Table IV.

Base is best on Japanese and second best on Korean for the books-vertical test set. However, on Chinese Traditional it performs so poorly that the mean script identification error on the domain is twice that of Gate and Max.

Photo data is inherently more challenging than books data which tends to be cleaner and less distorted. When the script is given, character recognition error rate is 2.5 to 5 times higher in photos than in books, as shown in the Oracle column. For example, Latin has 10.5% error rate in photos, 4.1% in books. Cyrillic has the largest difference between photos (11.4%) and books (2.2%). We plan to get more photo training data to reduce this gap.

Script identification error rates for Latin are remarkably lower than the other 4 scripts in the photos category. We believe this is primarily caused by the presence of real photo-like Latin training data. When we remove this data, the script

identification error rate for Gate summarizer on the Latin data set increases to 7%. We expect that adding photo-like script identification training data for other scripts will lower error rates further.

Photos result in aggregate agree with overall results. Compared to Base, Gate reduces script identification error rate by 12.5% relative (from 17.6% to 15.4%). The impact on end-to-end character recognition error is a 32% relative reduction, from 8.2% to 5.6%.

Cyrillic is an outlier. It has 11.0% end-to-end error rate with best script identification on top of 11.4% OCR error rate for Oracle-script. Base error is high on Cyrillic photos. The 49.5% script identification error rate is caused by Latin-looking characters having equal weight as distinctive Cyrillic characters in the voting heuristic of Base. Gate is better able to ignore confusable characters (more precisely, non-script-informative feature elements) through its attention mechanism.

VI. DISCUSSION

Fig. 8 visualizes the activation maps of Gate, Mean and Max summarizers. The activation map of $L(\mathbf{h})$ looks different for each summarizer. This indicates that each summarizer exerts distinct requirements on $L(\mathbf{h})$. The Mean activation map is fuzzier than for other summarizers. This makes sense considering that the Mean summarizer essentially performs voting. Even small values contribute to the final decision. In contrast, the Max summarizer produces the sharpest activation map. This makes sense since the Max summarizer considers only the strongest signal for each script. The Gate summarizer lies between the two in terms of the sharpness of the activation map. The gating mechanism (top rectangle \mathbf{g}) suppresses regions where the characters are not Cyrillic. It considers only relevant regions of the input. For instance, the activation map of $L(\mathbf{h})$ has activity on digits and the Latin-like character “a”. However, the activation map of \mathbf{g} suppresses this activity and highlights distinctive Cyrillic characters. This illustrates why the Gate summarizer performed so well. In principle LSTM should be able to learn a similar rule to Gate. However, our results do not bear that out. Understanding what is going inside the LSTM seems difficult. This is perhaps another advantage of Gate.

The experimental results show limitations of our approach. Except for Latin, OCR error rates double compared to the Oracle case on the challenging photo dataset. We believe that this is explained by the lack of photo training data for non-Latin languages, as discussed in Section V. Photos are harder for a number of reasons. Images have text facing sideways or with deep perspective vanishing point. Characters are partially occluded, upside down, blurry, or printed on wrinkly clothing.

When script identification fails, text recognition fails. The characters of one script are not usually supported by another script model. Even when characters from different scripts look similar their Unicode codepoints are different. For example, some Cyrillic characters look similar to Latin. One way to alleviate this problem is to consider multiple hypotheses when selecting models. Eq. (1) uses max to select the best script and

¹Full confusion matrices in <http://arxiv.org/abs/1708.04671>.

domain	script	Script ID Error Rate %					OCR Error % due to Script ID					Oracle-script OCR Err%
		Base	Gate	LSTM	Mean	Max	Base	Gate	LSTM	Mean	Max	
photos	Latn	1.0	1.2	0.8	0.8	1.4	0.8	0.8	0.8	0.8	0.9	10.5
	Cyrl	49.5	28.7	33.5	35.1	30.8	28.0	11.0	13.0	14.5	12.4	11.4
	Jpan	25.5	30.1	39.7	31.2	30.4	8.5	12.3	15.5	13.5	11.2	21.1
	Arab	19.0	23.5	26.7	26.0	27.7	6.8	7.0	7.4	7.9	9.0	15.0
	Deva	17.6	22.9	21.5	27.9	23.7	4.5	6.2	5.5	7.8	7.2	16.3
	Mean	17.6	15.4	17.7	17.5	16.5	8.2	5.6	6.4	6.7	6.1	13.3
books vertical	Hant	8.9	0.3	1.6	1.3	1.1	1.5	0.0	0.2	0.1	0.1	10.5
	Jpan	3.1	3.4	3.6	4.0	3.2	0.2	0.2	0.2	0.3	0.4	6.1
	Kore	2.9	4.1	4.8	5.2	1.4	1.0	1.7	2.1	2.0	0.5	7.3
	Mean	5.4	2.3	3.0	3.2	2.0	0.9	0.4	0.6	0.6	0.3	8.1
books horizontal	Latn	0.4	1.1	1.1	0.9	1.6	0.9	1.0	1.1	1.0	1.2	4.1
	Cyrl	3.6	1.3	2.2	2.4	1.9	2.4	0.7	1.2	1.5	1.3	2.2
	Deva	0.9	1.0	1.0	1.2	1.1	0.2	0.2	0.3	0.4	0.3	5.7
	Arab	0.9	1.1	1.7	1.6	1.8	0.2	0.3	0.4	0.4	0.6	6.6
	Tibt	2.4	2.9	3.2	2.4	3.1	1.4	1.7	1.6	1.2	1.9	4.7
	Syrc	4.4	4.6	4.5	4.7	6.0	1.2	1.4	1.3	1.3	2.0	1.9
	Hebr	0.2	0.1	0.3	0.4	0.1	0.1	0.1	0.2	0.2	0.1	5.2
	Ethi	1.0	1.3	2.9	2.2	2.4	0.5	0.7	1.2	0.9	1.1	0.5
	Geor	0.7	1.0	1.6	1.1	1.7	0.4	0.7	1.1	0.7	1.2	0.4
	Cher	5.2	3.5	4.3	3.1	5.0	3.9	2.6	3.4	2.2	3.5	0.4
	Beng	3.2	3.1	3.0	3.3	3.1	0.9	0.8	0.7	0.9	1.0	5.0
	Mymr	1.5	1.7	1.8	1.6	2.1	0.4	0.7	0.7	0.6	0.8	4.1
	Sinh	1.2	1.6	1.2	1.4	1.5	0.3	0.5	0.2	0.3	0.4	9.2
	Orya	5.0	4.0	2.8	4.1	5.7	2.7	1.5	1.3	1.9	2.3	6.0
	Thaa	0.7	0.6	1.4	0.8	0.7	0.3	0.1	0.4	0.1	0.2	1.1
	Laoo	6.7	4.6	8.9	4.1	9.6	2.1	1.2	3.5	1.1	4.5	14.6
	Gujr	1.0	0.4	0.6	0.8	0.5	0.5	0.3	0.3	0.4	0.3	7.4
	Guru	4.7	4.3	4.3	4.1	4.3	2.4	2.3	2.3	2.3	2.0	7.9
	Telu	1.0	0.4	0.6	1.0	0.3	0.4	0.2	0.2	0.2	0.2	7.7
	Knda	1.0	0.7	0.3	0.5	0.9	0.4	0.3	0.0	0.1	0.3	12.8
	Khmr	18.6	7.9	11.2	15.3	20.6	7.3	1.8	2.6	5.4	8.3	31.6
	Mlym	1.2	0.1	0.2	0.5	0.6	1.0	0.0	0.1	0.2	0.5	5.7
	Thai	0.3	0.4	0.1	0.3	0.8	0.2	0.3	0.1	0.4	0.6	3.1
	Armnr	21.2	2.6	3.7	12.2	6.1	15.8	1.3	1.9	8.5	3.4	4.2
	Taml	3.4	0.4	0.5	1.4	1.0	2.2	0.2	0.2	0.6	0.7	5.8
	Grek	12.4	1.4	1.6	1.2	2.9	9.1	1.0	1.1	0.7	2.0	4.8
	Kore	1.3	0.3	0.6	0.7	0.1	0.5	0.1	0.1	0.2	0.0	2.5
	Hans	1.8	5.3	6.2	2.9	4.8	0.1	0.5	1.0	0.2	0.6	2.4
	Jpan	8.2	7.2	7.5	10.1	7.0	0.8	0.6	0.6	1.1	0.6	4.9
	Hant	6.0	2.1	2.5	5.4	4.4	1.1	0.2	0.3	0.7	0.7	2.8
	Mean	1.9	1.5	1.8	1.8	2.2	1.3	0.9	1.0	1.0	1.2	4.4
Overall line-weighted mean		3.7	3.1	3.6	3.5	3.8	2.1	1.4	1.6	1.7	1.8	5.5

TABLE IV
RESULTS



Fig. 8. Visualization of the activation maps of Gate, Mean and Max summarizers. Brighter pixels mean greater values. Each row corresponds to a script. The input image is in Cyrillic script and obtained from the photo dataset. For this particular example, Gate and Max correctly predict the script while Mean mispredicts it as Latin. The gating mechanism allows for Gate to attend to Cyrillic characters (e.g. the second to last character) and ignore irrelevant characters such as digits.

makes a hard decision. Instead, we could try several per-script OCR models. This introduces a trade-off between computation effort and accuracy. Another approach is to design an end-to-end text recognition system that embeds script identification. Likely many of the features used for OCR can be reused for

script identification and only be computed once.

In our approach we take an entire text line as the unit for script classification. A line image is a natural unit for an OCR system from a text-detection and layout-analysis point of view. In addition it presents sufficient context for the newest

sequence to sequence recognizers to deliver good accuracy by taking into account a language model. The vast majority of lines encountered many documents and use-cases will contain only a single language. This motivated the decision in the prior work [1] to aggregate script identification at the line-level via a counting heuristic. Nevertheless, a multilingual OCR system should ideally be able to handle arbitrary mixed-script and mixed-language content. One way to deal with this problem [1], [16] is by detecting scripts at finer levels. Another way is to keep the line-level approach and consider multiple scripts in Eq. (1). The post-recognition layout analysis phase in Fig. 1 removing can then remove overlapping words. It may however be preferable to have a system that handles multiscript lines directly.

We addressed the script identification problem by framing it as a sequence-to-label problem. This formulation is generic and can be applied to other use cases. For example, line orientation-direction detection can find the orientation and reading order of text. Another use case is garbage detection which determines if the input line is text or not, as a filter for later stages.

VII. CONCLUSION

We considered line-level script identification in the context of multilingual OCR, where a script identification step selects the script-specific model used by the OCR engine. We investigated several variants of an *encoder-summarizer* approach in the context of a state-of-the-art multilingual OCR system. We used an evaluation set of multiple-domain line images in 30 scripts from 232 languages. We compared this approach against a well-performing but expensive prior baseline [1]. We found that the best variants of the new approach improve significantly over the baseline. In addition the approach offers computational advantage. The most promising variant is the *Gate* system. It uses learned attention to emphasize salient features. It reduces script identification errors by 16%, and character recognition error rates from script misidentification by a third.

We also discussed a limitation of our approach: the inability to handle multiple scripts within a line. Dealing with such cases using a single model is future work.

ACKNOWLEDGMENT

The authors would like to thank Thomas Deselaers, Reeve Ingle, Sergey Ioffe, Henry Rowley, and Ray Smith for comments on early versions of this paper.

REFERENCES

- [1] D. Genzel, A. C. Popat, R. Teunen, and Y. Fujii, "HMM-based Script Identification for OCR," in *Proceedings of the 4th International Workshop on Multilingual OCR*, ser. MOCR '13. New York, NY, USA: ACM, 2013, pp. 2:1–2:5.
- [2] D. Ghosh, T. Dube, and A. Shivaprasad, "Script recognition—a review," *IEEE Trans. Pattern Anal. Mach. Intell.*, vol. 32, no. 12, pp. 2142–2161, Dec. 2010.
- [3] N. Sharma, U. Pal, and M. Blumenstein, "Recent advances in video based document processing: A review," in *Document Analysis Systems*. IEEE Computer Society, 2012, pp. 63–68.
- [4] B. Shi, C. Yao, and C. Zhang, "Automatic script identification in the wild," in *Proceedings of the 13th International Conference on Document Analysis and Recognition*. IEEE, Aug. 2015, pp. 976–980.
- [5] A. K. Singh and C. V. Jawahar, "Can rnns reliably separate script and language at word and line level?" in *Proceedings of the 13th International Conference on Document Analysis and Recognition*. IEEE, Aug. 2015, pp. 976–980.
- [6] K. Veselý, S. Watanabe, and K. Žmolková, "Sequence summarizing neural network for speaker adaptation," in *Proceedings of the 41st International Conference on Acoustics, Speech and Signal Processing (ICASSP)*. IEEE, Mar. 2016, pp. 5315–5319.
- [7] G. Heigold, I. Moreno, S. Bengio, and N. Shazeer, "End-to-end text-dependent speaker verification," in *Proceedings of the 41st International Conference on Acoustics, Speech and Signal Processing (ICASSP)*. IEEE, Mar. 2016, pp. 5315–5319.
- [8] C. Szegedy, W. Liu, Y. Jia, P. Sermanet, S. Reed, D. Anguelov, D. Erhan, V. Vanhoucke, and A. Rabinovich, "Going Deeper with Convolutions," in *Proceedings of Computer Vision and Pattern Recognition (CVPR)*, Jun. 2015.
- [9] R. Smith, "Hybrid page layout analysis via tab-stop detection," in *Proceedings of the 10th International Conference on Document Analysis and Recognition*. IEEE, Jul. 2009, pp. 241–245.
- [10] Y. Fujii, D. Genzel, A. C. Popat, and R. Teunen, "Label transition and selection pruning and automatic decoding parameter optimization for time-synchronous viterbi decoding," in *Proceedings of the 13th International Conference on Document Analysis and Recognition*. IEEE, Aug. 2015, pp. 756–760.
- [11] A. Graves, S. Fernández, F. Gomez, and J. Schmidhuber, "Connectionist temporal classification: Labelling unsegmented sequence data with recurrent neural networks," in *Proceedings of the 23rd International Conference on Machine Learning*. ACM, Jun. 2006, pp. 369–376.
- [12] H. A. Bourlard and N. Morgan, *Connectionist Speech Recognition: A Hybrid Approach*. Norwell, MA, USA: Kluwer Academic Publishers, 1993.
- [13] I. Sutskever, O. Vinyals, and Q. V. Le, "Sequence to sequence learning with neural networks," in *NIPS'14 Proceedings of the 27th International Conference on Neural Information Processing Systems*, Dec. 2014, pp. 3104–3112.
- [14] S. Hochreiter and J. Schmidhuber, "Long short-term memory," *Neural Comput.*, vol. 9, no. 8, pp. 1735–1780, Nov. 1997.
- [15] M. Abadi, P. Barham, J. Chen, Z. Chen, A. Davis, J. Dean, M. Devin, S. Ghemawat, G. Irving, M. Isard, M. Kudlur, J. Levenberg, R. Monga, S. Moore, D. G. Murray, B. Steiner, P. Tucker, V. Vasudevan, P. Warden, M. Wicke, Y. Yu, and X. Zheng, "Tensorflow: A system for large-scale machine learning," in *12th USENIX Symposium on Operating Systems Design and Implementation (OSDI 16)*, 2016, pp. 265–283.
- [16] A. Ul-Hasan, M. Z. Afzal, F. Shafait, M. Liwicki, and T. M. Breuel, "A sequence learning approach for multiple script identification," in *Proceedings of the 13th International Conference on Document Analysis and Recognition*. IEEE, Aug. 2015, pp. 1046–1050.

	Arab	Armn	Beng	Cher	Cyrl	Deva	Ethi	Geor	Grek	Gujr	Guru	Hans	Hant	Hebr	Jpan	Khmr	Knda	Kore	Lao	Latn	Mlym	Mymr	Orya	Sinh	Syrc	Taml	Telu	Thaa	Thai	Tibt
Arab	99.1	0	0	0	0	0	0	0	0	0	0	0	0	0	0	0	0	0	0	0.8	0	0	0	0	0	0	0	0	0	0
Armn	0	78.8	0	0	0	0	0	0	0	0	0	0	0	0	0	0	0	0	0	21.1	0	0	0	0	0	0	0	0	0	0
Beng	0	0	96.8	0	0	0.3	0	0	0	0	0	0	0	0	0	0	0	0	0	2.8	0	0	0	0	0	0	0	0	0	0
Cher	0	0	0	94.8	0	0	0	0	0	0	0	0	0	0	0	0	0	0	0	5.2	0	0	0	0	0	0	0	0	0	0
Cyrl	0	0	0	0	95.8	0	0	0	0	0	0	0	0	0	0	0	0	0	0	4.2	0	0	0	0	0	0	0	0	0	0
Deva	0	0	0	0	0	99.1	0	0	0	0	0	0	0	0	0	0	0	0	0	0.6	0	0	0	0	0	0	0	0	0	0
Ethi	0	0	0	0	0	0	99	0	0	0	0	0	0	0	0	0	0	0	0	0.9	0	0	0	0	0	0	0	0	0	0
Geor	0	0	0	0	0	0	0	99.3	0	0	0	0	0	0	0	0	0	0	0	0.5	0	0	0	0	0	0	0	0	0	0
Grek	0	0	0	0	0.1	0	0	0	87.6	0	0	0	0	0	0	0	0	0	0	12.3	0	0	0	0	0	0	0	0	0	0
Gujr	0	0	0	0	0	0.3	0	0	0	99	0	0	0	0	0	0	0	0	0	0.8	0	0	0	0	0	0	0	0	0	0
Guru	2.4	0	0	0	0	0.5	0	0	0	0	95.3	0	0	0	0	0	0	0	0	1.8	0	0	0	0	0	0	0	0	0	0
Hans	0	0	0	0	0	0	0	0	0	0	0	98.2	1.7	0	0	0	0	0	0	0.1	0	0	0	0	0	0	0	0	0	0
Hant	0	0	0	0	0	0	0	0	0	0	0	7.3	92	0	0.6	0	0	0	0	0	0	0	0	0	0	0	0	0	0	0
Hebr	0	0	0	0	0	0	0	0	0	0	0	0	0	99.8	0	0	0	0	0	0.2	0	0	0	0	0	0	0	0	0	0
Jpan	0	0	0	0	0	0	0	0	0	0	0	1.9	2.6	0	95.3	0	0	0	0	0.2	0	0	0	0	0	0	0	0	0	0
Khmr	0	0	0	0	0	0	0	0	0	0	0	0.2	0	0	0	81.4	0	0	0	15.7	0	0	0	0	0	0	0	0	2.6	0
Knda	0	0	0	0	0	0	0	0	0	0	0	0	0	0	0	0	99	0	0	0.4	0	0	0	0	0	0	0.5	0	0	0
Kore	0.1	0	0	0	0	0	0	0	0.1	0	0	0.1	1.3	0	0	0	0	97.9	0	0.5	0	0	0	0	0	0	0	0	0	0
Lao	0	0	0	0.2	0	0	0	0	0	0	0	0	0	0	0	0.6	0	0	93.3	3.5	0	0.8	0	0	0	0	0.6	0	0.9	0
Latn	0	0	0	0	0	0	0	0	0	0	0	0	0	0	0	0	0	0	99.7	0	0	0	0	0	0	0	0	0	0	0
Mlym	0	0	0	0	0	0	0	0	0	0	0	0	0	0	0	0	0	0	0	1.2	98.8	0	0	0	0	0	0	0	0	0
Mymr	0	0	0	0	0	0	0	0	0	0	0	0	0	0	0	0	0	0	0	1	0	98.5	0	0	0	0	0.1	0	0	0
Orya	0	0	0.1	0	0	0	0	0	0	0	0	0	0	0	0	0	0	0	0	4.4	0	0	95	0	0	0	0	0	0	0
Sinh	0	0	0	0	0	0	0	0	0	0	0	0	0	0	0	0	0.2	0	0	0.7	0	0	0	98.8	0	0	0.1	0	0	0
Syrc	1.2	0	0	0	0	0	0	0	0	0	0	0	0	0	0	0	0	0	0	2.9	0	0	0	0	95.6	0	0	0	0	0
Taml	0	0	0	0	0	0	0	0	0	0	0	0	0	0	0	0	0	0	0	3.4	0	0	0	0	0	96.6	0	0	0	0
Telu	0	0	0	0	0	0	0	0	0	0	0	0	0	0	0	0	0	0	0	1	0	0	0	0	0	0	99	0	0	0
Thaa	0.2	0	0	0	0	0	0	0	0	0	0	0	0	0	0	0	0	0	0	0.5	0	0	0	0	0	0	0	99.3	0	0
Thai	0	0	0	0	0	0	0	0	0	0	0	0	0	0	0	0	0	0	0	0.3	0	0	0	0	0	0	0	0	99.7	0
Tibt	0.1	0	0	0	0	0.1	0	0	0	0	0.3	0	0	0	0	0	0	0	0	1.3	0	0	0	0	0.2	0	0	0	0	97.6

TABLE V
FULL CONFUSION MATRIX FOR BASE

	Arab	Armn	Beng	Cher	Cyrl	Deva	Ethi	Geor	Grek	Gujr	Guru	Hans	Hant	Hebr	Jpan	Khmr	Knda	Kore	Lao	Latn	Mlym	Mymr	Orya	Sinh	Syrc	Taml	Telu	Thaa	Thai	Tibt
Arab	98.9	0	0	0	0	0	0	0	0	0	0	0	0	0	0	0	0	0	0	0.4	0	0	0	0.1	0	0	0	0	0	0
Armn	0	97.4	0	0	0	0	0	0	0	0	0	0	0	0	0	0	0	0	0	2.3	0	0	0	0	0	0	0	0	0	0
Beng	0	0	97	0	0	0.6	0	0	0	0	0.2	0	0	0	0	0	0	0	0	1.6	0	0	0	0.1	0	0	0	0	0	0
Cher	0	0	0	96.3	0.2	0	0.1	0	0	0	0	0	0	0	0	0	0	0	0	2.6	0	0	0	0	0	0	0	0	0.1	0
Cyrl	0	0	0	0	98	0	0	0	0	0	0	0	0	0	0	0	0	0	0	1.8	0	0	0	0	0	0	0	0	0	0
Deva	0	0	0	0	0	99	0	0	0	0	0.2	0.1	0	0	0	0	0	0	0	0.2	0	0	0	0	0	0	0	0	0	0
Ethi	0	0	0	0	0	0	98.6	0	0	0	0	0.2	0	0	0	0	0	0	0	0.7	0	0	0	0	0	0	0	0	0	0
Geor	0	0	0	0	0	0	0	99	0	0	0	0	0	0	0	0	0	0	0	0.5	0	0	0	0	0	0	0	0	0	0
Grek	0	0	0	0	0	0	0	0	98.1	0	0	0	0	0	0	0	0	0	0	1.4	0	0	0	0	0	0	0	0	0	0
Gujr	0	0	0	0	0	0.3	0	0	0	99.6	0	0	0	0	0	0	0	0	0	0.2	0	0	0	0	0	0	0	0	0	0
Guru	2.5	0	0	0	0	0.6	0	0	0	0	95.7	0	0	0	0	0	0	0	0	1.1	0	0	0	0	0	0	0	0	0	0
Hans	0	0	0	0	0.2	0	0	0	0	0	0	95	3.7	0	0.8	0	0	0	0	0.2	0	0	0	0	0	0	0	0	0	0
Hant	0	0	0	0	0	0	0	0	0	0	0	0.8	99.1	0	0	0	0	0	0	0	0	0	0	0	0	0	0	0	0	0
Hebr	0	0	0	0	0	0	0	0	0	0	0	0	0	99.9	0	0	0	0	0	0	0	0	0	0	0	0	0	0	0	0
Jpan	0	0	0	0	0	0	0	0	0	0	0	0.6	3.9	0	95.4	0	0	0	0	0	0	0	0	0	0	0	0	0	0	0
Khmr	0	0	0	0	0	0	0.2	0	0	0	0	0	0	0	0	92.1	0.2	0	1.7	5.5	0	0	0	0	0	0	0	0	0.3	0
Knda	0	0	0	0	0	0	0	0	0	0	0	0	0	0	0	0	99.3	0	0	0	0	0	0	0	0	0	0.6	0	0	0
Kore	0	0	0	0	0	0	0	0	0	0	0.2	0.3	1.2	0	0	0	0.1	97.7	0	0.3	0	0	0	0	0	0	0	0	0	0
Lao	0	0	0	0	0	0	0	0	0	0	0	0	0	0.2	0	0.7	0	0	95.4	1.6	0	0.4	0	0	0	0	1.4	0	0.3	0
Latn	0	0	0	0	0.4	0	0	0	0	0	0	0	0	0	0	0	0	0	0	98.8	0	0	0	0	0	0	0	0	0	0
Mlym	0	0	0	0	0	0	0	0	0	0	0	0	0	0	0	0	0	0	0	0	99.9	0	0	0	0	0	0	0	0	0
Mymr	0	0	0	0	0.1	0	0	0	0	0	0	0	0	0	0	0	0	0	0.1	0.2	0.2	98.4	0.1	0	0	0	0.2	0	0	0
Orya	0	0	0	0	0.3	0	0	0	0	0	0.2	0	0.1	0	0	0.4	0	0	0	2.2	0	0.2	96	0	0	0	0	0	0	0
Sinh	0	0	0	0	0	0	0	0	0	0	0.2	0.1	0	0	0	0	0.1	0	0	0.6	0	0	0.1	98.4	0	0	0	0	0	0
Syrc	0.9	0	0	0	0	0	0	0	0	0	0.3	0	0	0.2	0	0	0	0	0	1.2	0.1	0	0	0	95.4	0	0.1	0	0	0.3
Taml	0.1	0	0	0	0	0	0	0	0	0	0	0	0	0	0	0	0	0	0	0.3	0	0	0	0	0	99.6	0	0	0	0
Telu	0	0	0	0	0	0	0.2	0	0	0	0	0	0	0	0	0	0	0	0	0.3	0	0	0	0	0	0	99.6	0	0	0
Thaa	0	0	0	0	0	0	0	0	0	0	0	0	0	0	0	0	0	0	0	0	0	0	0	0	0	0	0	99.4	0	0
Thai	0	0	0	0	0	0	0	0	0	0	0	0	0	0	0	0	0	0	0	0.2	0	0	0	0	0	0	0	0	99.6	0
Tibt	0	0	0	0	0	0.3	0	0	0	0	0.5	0	0	0	0	0.1	0	0	0	0.3	0	0	0	0	0.2	0	0	0	0	97.1